

# Twenty barrel *in situ* pipe gun type solid hydrogen pellet injector for the Large Helical Device

Cite as: Rev. Sci. Instrum. **84**, 083504 (2013); <https://doi.org/10.1063/1.4816823>

Submitted: 09 May 2013 • Accepted: 15 July 2013 • Published Online: 07 August 2013

Ryuichi Sakamoto, Gen Motojima, Hiromi Hayashi, et al.



View Online



Export Citation



CrossMark

## ARTICLES YOU MAY BE INTERESTED IN

### [Pellet injection technology](#)

Review of Scientific Instruments **64**, 1679 (1993); <https://doi.org/10.1063/1.1143995>

### [Measuring fast electron spectra and laser absorption in relativistic laser-solid interactions using differential bremsstrahlung photon detectors](#)

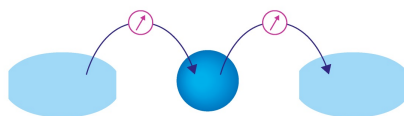
Review of Scientific Instruments **84**, 083505 (2013); <https://doi.org/10.1063/1.4816332>

### [Bayesian soft X-ray tomography using non-stationary Gaussian Processes](#)

Review of Scientific Instruments **84**, 083506 (2013); <https://doi.org/10.1063/1.4817591>

Webinar

Interfaces: how they make  
or break a nanodevice



March 29th – Register now



Zurich  
Instruments



## Twenty barrel *in situ* pipe gun type solid hydrogen pellet injector for the Large Helical Device

Ryuichi Sakamoto,<sup>a)</sup> Gen Motojima, Hiromi Hayashi, Tomoyuki Inoue, Yasuhiko Ito, Hideki Ogawa, Shigeyuki Takami, Mitsuhiro Yokota, and Hiroshi Yamada  
*National Institute for Fusion Science, Toki, Gifu 509-5292, Japan*

(Received 9 May 2013; accepted 15 July 2013; published online 7 August 2013)

A 20 barrel solid hydrogen pellet injector, which is able to inject 20 cylindrical pellets with a diameter and length of between 3.0 and 3.8 mm at the velocity of 1200 m/s, has been developed for the purpose of direct core fueling in LHD (Large Helical Device). The *in situ* pipe gun concept with the use of compact cryo-coolers enables stable operation as a fundamental facility in plasma experiments. The combination of the two types of pellet injection timing control modes, i.e., pre-programming mode and real-time control mode, allows the build-up and sustainment of high density plasma around the density limit. The pellet injector has demonstrated stable operation characteristics during the past three years of LHD experiments. © 2013 AIP Publishing LLC. [<http://dx.doi.org/10.1063/1.4816823>]

### I. INTRODUCTION

Core fueling becomes increasingly important in a future fusion reactor in which a magnetically confined burning plasma is sustained by its own  $\alpha$  particle heating. Pellet fueling that injects cryogenic hydrogen pellets into the core plasma directly at high speeds is one of the few means of supplying fueling particles into the high-temperature burning plasma. Pellet injection has been being investigated for the past 40 years, and many studies have indicated that pellet injection contributes not only to efficient fueling but also to improvements in plasma confinement properties.<sup>1-3</sup> On the other hand, because it is not necessary to consider the burnout of fuel in the present plasma experiments, fueling is still not considered as an important issue. And therefore, it remains as a big issue to be resolved despite its importance.

In order to confirm the adequacy of the pellet fueling to the high temperature plasma, pellet fueling experiments are intensively investigated in the LHD (Large Helical Device) which is world's largest helical system with superconducting magnets.<sup>4</sup> Since external coils generate the entire confinement field, plasma current is not required to sustain the plasma and therefore there is an excellent adaptability to high density operation in helical systems. One of the significant results of high density operation in the LHD is the formation of an IDB (Internal diffusion Barrier).<sup>5</sup> The IDB is formed in intensive multi-pellet-fueled high density discharges, and characterized by steep density gradients and very high pressure in the core region up to 150 kPa.<sup>6</sup> In the previous experiments, the IDB plasma is transiently formed by using the existing 10 barrel pellet injector,<sup>7</sup> however, it cannot sustain the high density plasma with the IDB due to the lack of pellets to supply the particles. In order to investigate the long-duration sustainability of the pellet fueled high performance plasma with the IDB, additional pellet injection capability is required. Already we had developed a repetitive pellet injector with a screw type solid hydrogen extruder which can inject pellets continuously

at a frequency of up to 11 Hz.<sup>8</sup> However, its core fueling capabilities are far from adequate to build up the highly peaked IDB plasmas due to deficiencies in maximum pellet velocity and minimum pellet injection interval. From the view point of the core fueling capabilities, a simple *in situ* pipe gun type solid hydrogen pellet injector is preferable although the possible number of pellet injections is exactly restricted by the installed number of pellet injection barrels. Above-mentioned facts motivated us to develop a 20 barrel *in situ* pipe gun type solid hydrogen pellet injector. The pellet injector design has the largest number of barrels ever along with the 20 barrel pellet injector in the Alcator C-Mod.<sup>9</sup>

In this paper, we would like to introduce the newly developed 20 barrel *in situ* pipe gun type solid hydrogen pellet injector in the LHD. The requirements and design overview of the pellet injector are indicated in Sec. II. A performance of each component of the pellet injector is described in Sec. III. The first application results of the pellet injector on the LHD are shown in Sec. IV.

### II. REQUIREMENTS AND DESIGN OVERVIEW

In the LHD, plasma experiments are carrying out every 3 min for 9 h per day, and entry to the LHD experimental hall is not allowed throughout the day. The following requirements, therefore, must be met by the pellet injector, (1) reliability and stability as a fundamental facility that is ready for use at any time during the plasma experiments, and (2) fully remote control capability without any access for several months-long experiment. And there are additional requirements from the viewpoint of the experiments; (3) sufficient amount of particle supply for high density discharges with 10 s pulse width; and (4) flexibility to cope with experimental requirements that change according to the situation, e.g., changing pellet size and velocity.

In order to secure the reliability and stability, a conventional *in situ* pneumatic pipe gun concept<sup>10</sup> was adopted for a basic design in the same manner as the previous pellet injector in LHD.<sup>11</sup> The *in situ* pneumatic pipe gun has no movable

<sup>a)</sup>Electronic mail: sakamoto@LHD.nifs.ac.jp

components in the cryogenic part and the pellet size is fixed by the inner radius of an injection barrel. These features allow reliable operation, however, only one pellet injection is available from each barrel. Therefore, it is required to arrange enough barrels in order to inject multiple pellets in a plasma discharge. This is a definite disadvantage of the *in situ* pneumatic pipe gun, but at the same time, it leads to flexibility to change the pellet injection conditions, especially pellet size, with respect to each barrel because the pellets are injected using individual barrels. It is assumed that 20 barrels are required to sustain a high density discharge for 10 s pulse width in LHD. First 3–10 pellets are intensively injected to form a high density plasma,<sup>6</sup> and the other remaining pellets are used to sustain the high density plasma.

The pellet size and velocity are determined semi-empirically by the previous experimental result and by a model calculation using the NGS (neutral gas shielding) model<sup>12</sup> which is widely accepted pellet ablation model. The pellet sizes are decided as 3.8 mm (four pellets), 3.4 mm (six pellets), and 3.0 mm (ten pellets) in diameter and length with cylindrical shape. The particle numbers in each size of pellet are approximately  $2.0 \times 10^{21}$ ,  $1.5 \times 10^{21}$ , and  $1.0 \times 10^{21}$ , respectively. Although pellet velocity is an important factor to decide the fueling property, the range of the available velocity is generally restricted from 800 m/s to 1200 m/s in the case of a single stage pneumatic pipe gun type pellet injector. The maximum velocity is restricted by the sound velocity of the propellant gas and the minimum one is restricted by the minimum pressure to break away a sticking pellet from the barrel. This pellet injector is designed to achieve higher velocity within reasonable limits. A contour plot of the pellet penetration depth dependence on the electron temperature,  $T_e$ , and pellet velocity,  $V_p$ , which is predicted by the NGS model under a typical LHD plasma condition, is shown in Fig. 1. The pellet penetration depth strongly depends on  $T_e$ . The effect of the size and velocity variations are relatively weak and the penetration depth is almost the same level within the available pellet size and velocity ranges between 3.0 and 3.8 mm and between 800 and 1200 m/s, respectively. The estimated pellet penetration depth reaches around the magnetic axis in the typical temperature range of high density discharges between 1.0 and 2.0 keV.

Although the pellet injection timing control becomes important especially in high density discharges around the density limit, it is very difficult to decide the adequate pellet injection timing, which is necessary to sustain the high density plasma avoiding a radiation collapse, before the discharge. In order to solve this problem, it is required to control the pellet injection timing in real time referring to a density related measurement, e.g., interferometer or bremsstrahlung, in addition to a pre-programmed injection timing control.

A fully remote control capability is secured by employing GM (Gifford-McMahon) cycle compact cryo-coolers as with the previous pellet injectors which are developed for the LHD experiments.<sup>8,11</sup> Since the pellet injector can be operated by using only electric power, which is the most fundamental facility in a laboratory, without a liquid helium supply system; it is possible to operate the pellet injector remotely without accessing it for a long time.

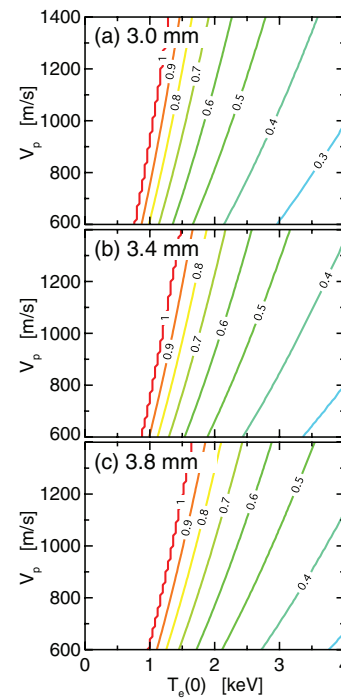


FIG. 1. Contour plots of the normalized pellet penetration depth:  $\lambda a$  for each pellet size, cylindrical shape with (a) 3.0 mm, (b) 3.4 mm, and (c) 3.8 mm in diameter and length, predicted by NGS pellet ablation model. Flat density profile:  $n_e = 5 \times 10^{19} (1 - (\frac{\rho}{1.1})^{14})^2 \text{ m}^{-3}$  and parabolic temperature profile:  $T_e = T_e(0)(1 - \frac{\rho}{1.1})^2 \text{ keV}$ , where  $T_e(0) = 0\text{--}4 \text{ keV}$ , are assumed.  $\lambda a = 1$  represents that the pellet penetrates to the plasma center:  $\rho = 0$ .

The cabling distance between the LHD main control room and the LHD experimental hall is about 400 m. In order to minimize the cabling, the remote control of the pellet injector has been built on an Ethernet connection with the fiber optics between the control computers in the LHD main control room and the PLC (Programmable Logic Controllers) located near the pellet injector in the LHD experimental hall.

In order to secure the flexibility to adapt to changes accompanying the progress of the experiments, the injection barrels are designed such that the size can be changed easily. The control software is built with a general-purpose language, and it can be changed on demand with the progress of the experiment.

### III. COMPONENTS OF THE SYSTEM

Fig. 2 shows an external drawing of the pellet injector. The screw-extruder type repetitive pellet injector<sup>8</sup> is installed behind the 20 barrel *in situ* pneumatic pipe gun type pellet injector to share the differential pumping system. However, the repetitive pellet injector is beyond the scope of this paper. The *in situ* pneumatic pipe gun pellet injector is divided roughly into the following two parts with different functions. One is a pellet formation/acceleration part which consists of a cryostat and valve set. This part is the main part of the pellet injector. Another is a differential pumping system with three pumping stages, which is connected in series with narrow guide tubes. The function of the differential pumping system is to

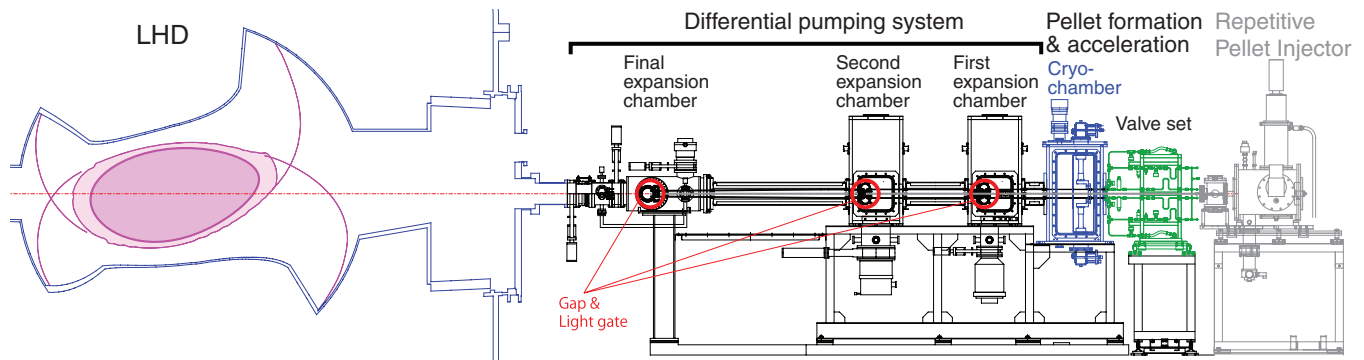


FIG. 2. Schematic view of the 20 barrel *in situ* pipe gun type solid hydrogen pellet injector and the LHD plasma. The pellet injector is installed at the vicinity of horizontally elongated poloidal cross section on the outboard side mid-plane.

evacuate propellant gas, which is used for accelerating pellets, to minimize the inflow of gas into the LHD vacuum vessel.

### A. Formation and acceleration of a solid hydrogen pellet

The pellet injector has 20 barrels in total, four 3.8 mm barrels, six 3.4 mm barrels, and ten 3.0 mm barrels. The barrels are made of bright annealing 316 austenite stainless steel pipes. A thin-walled pipe (0.3 mm) is employed to prevent heat transfer along the barrel into the cryogenic part. A copper block is brazed in vacuum by palladium filler as shown in Fig. 3(a). The brazing width is the same as the inner diameter of the barrel to form the cylindrical solid hydrogen, which has equal lengths for the diameter and height.

By mechanically (using an M16 thread) connecting the copper block to the cryogenic heat sink, which is cooled by the second stage of the GM cycle cryo-cooler (SHI RDK-415D; 1.5 W@4 K), the pellet formation part in the barrel is cooled down. Solid hydrogen can be formed below the triple point temperature (13.8 K), and it has been indicated that a lower temperature is preferable from the view point of the strength of solid hydrogen which has an effect on the quality and velocity of the pellet.<sup>13</sup> The pellet injector, therefore, is operated at the attainable minimum temperature without any temperature control. The effective operational temperature is at  $\sim 5$  K in the stand-by phase and at  $\sim 7$  K during the continuous full operation phase. Five barrels are connected to a cryo-cooler through the cryogenic heat sink. A full depth slit with 3 mm width and 50 mm length is made between the barrels adjacent to each other at the timing of the pellet injection. The four sets of cryogenic heat sinks constitute the 20 barrels as shown in Fig. 3(b). These four sets of cryogenic heat sinks are surrounded by a thermal shield, which is made of thin copper plate with nickel plating, to prevent radiative heat transfer from the inner wall of the cryostat, and the thermal shield is connected to the first stages (40 W@40 K per a cryo-cooler) of the four cryo-coolers as shown in Fig. 3(c).

Negative temperature coefficient thin film resistance cryogenic temperature sensors (Lakeshore CERNOX) are installed at the far-end from the cold head in each cryogenic

heat sink and thermal shield. Only hydrogen (protium) is used as a fuel gas in LHD experiments. Since the triple-point temperature of hydrogen gas is relatively low as compared to deuterium, active temperature control using a heater is not necessary and the pellet injector is operated at the minimum temperature, which is automatically decided by a heat balance, as previously mentioned. In case, however, a deuterium pellet is required in the future, it may be necessary to control the pellet formation temperature owing to the rise of the triple-point temperature. Fig. 4 shows the cooling characteristics of the cryogenic heat sinks which have a weight of about 24 kg in total. The cooling down time from room temperature to the operational temperature (5 K) is about 6.5 h. The temperature rise 12 h after stopping the cryo-coolers is about 110 K, and the re-cooling down time from the temperature to the operational temperature is about 1 h. Therefore, the effective preparation time before pellet injection is 1 h during the experimental campaign.

The valve set to control pellet formation and acceleration is shown in Fig. 3(c). There are five valves per barrel, V1, V2, and V3 are pneumatic stopping valves, Vn is a micro-flow-regulating valve and Vf is a fast pulse valve. Hydrogen gas flows into the barrel by opening V1 and V2. The flow rate of hydrogen gas is tuned to approximately  $0.1 \text{ Pa m}^3/\text{s}$  beforehand by Vr. Hydrogen gas condenses on the cooling zone of the barrel inner wall, and a cylindrical solid hydrogen pellet is formed within 60 s. Although the diameter of the pellet is fixed to the inner diameter of the barrel, the length of the pellet can be controlled up to a 1.7-fold by reducing the temperature gradient along the barrel.<sup>14</sup> The minimum pellet size, namely, where the pellet length is the same as the pellet diameter, is chosen here by making a large temperature gradient. After forming a pellet, residual hydrogen gas inside the barrel is exhausted by closing V2 and opening V3. Then all valves are closed awaiting the injection trigger. Getting the injection trigger, Vf is opened for a short time ( $< 1.2$  ms), and then high pressure propellant gas flows into the barrel and the pellet is accelerated by the expanding propellant gas. Each and every barrel is controlled independently as is the case with the above control procedure.

The pellet velocity and mass have an effect on the fueling properties (e.g., penetration depth and density increment,



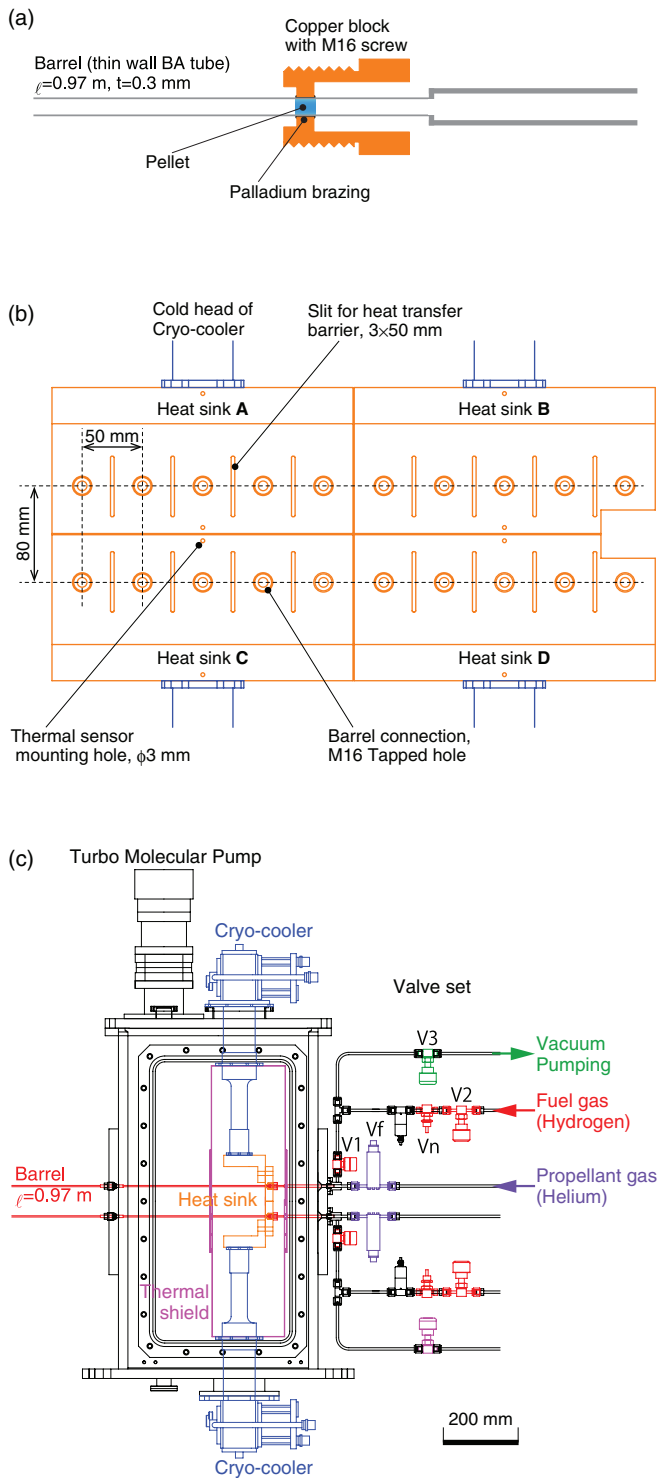


FIG. 3. Schematic view of the pellet formation part in the cryogenic chamber. (a) The enlarged illustration of the pellet formation part in the barrel. The barrel which is made of bright annealing 316 austenite stainless steel pipe is brazed with the oxygen-free copper block. (b) Arrangement of four sets of heat sinks viewed from the rear face. Five barrels are mechanically connected by M16 threads to a heat sink which is cooled by the exclusive compact cryo-cooler. (c) Side view of the cryogenic chamber and valve set.

respectively), however the pellet mass cannot be decided freely because it has a direct affect on the density increment. The pellet velocity, therefore, is the only free parameter to control pellet fueling properties. The pneumatically accelerated pellet velocity is described by Eq. (1) supposing the ideal

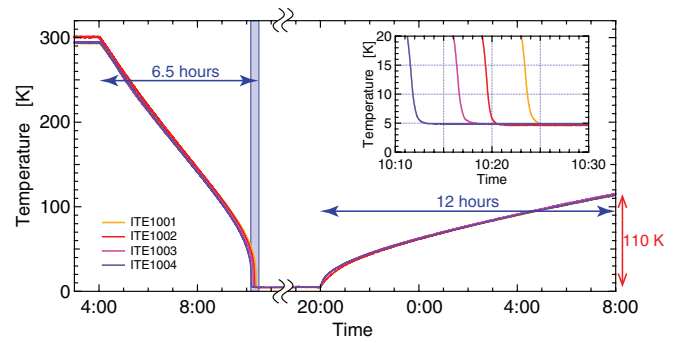


FIG. 4. Typical cooling down characteristics of the cryogenic heat sinks. The enlarged plot around the completion of the cooling down that is indicated by colored band is also plotted.

propagation of a one-dimensional rarefaction wave<sup>15</sup>

$$U(t) = \frac{2C_0}{\gamma - 1} \left[ 1 - \left( 1 + \frac{(\gamma + 1)P_0}{2d\rho_s C_0} t \right)^{-\frac{\gamma-1}{\gamma+1}} \right], \quad (1)$$

where  $U(t)$ ,  $d$ ,  $P_0$ ,  $\gamma$ ,  $\rho_s$ ,  $C_0$ , and  $t$  denote the pellet velocity, diameter of cylindrical pellet, initial pressure of propellant gas, specific heat ratio of propellant gas, solid hydrogen density, sound velocity of propellant gas ( $=\sqrt{\gamma kT/m}$ ) and acceleration time in the barrel, respectively. Although hydrogen gas is preferable to obtain higher velocity, helium gas is employed as a propellant gas for safety reasons here. The initial pressure of the propellant gas,  $P_0$ , and the barrel length,  $L_0$ , which is obtained by integrating  $U(t)$  over the acceleration time, are arbitrary design parameters. Fig. 5(a) shows the barrel length dependence of the predicted pellet velocity. Although the pellet velocity increases as the barrel length gets longer, the increase in rate becomes less significant, and

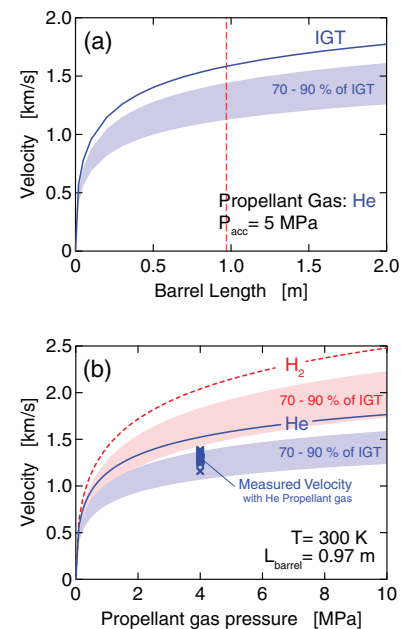


FIG. 5. Predicted pellet velocity by the ideal gun theory. Lines and colored bands denote the calculated values and semi-empirically predicted ranges of the pellet velocity, respectively. (a) Barrel length dependence for 5 MPa He propellant gas. (b) Propellant gas pressure dependence at the barrel length of  $L_{\text{barrel}} = 0.97$  m. Hydrogen and helium are considered as propellant gases.

therefore it is necessary to find an acceptable compromise. The barrel length is taken as 0.97 m considering the maximum length that is acceptable by the device geometry. Initial propellant gas pressure dependence of the pellet velocity is shown in Fig. 5(b). The theoretical predicted values and experimental values are denoted by a solid line and cross symbols, respectively. The experimental velocity is about a 15% reduction from the theoretical prediction. This tendency is the same level as that of other pellet injectors.<sup>3</sup>

The launched pellet is transferred to the LHD vacuum vessel through a guide tube, which penetrates expansion chambers of the differential pumping system. The guide tube has a 20 mm gap at center of each expansion chamber to release the spent propellant gas (see Sec. III B). At the gap, the inner diameter of the downstream guide tube is larger than that of the upstream one taking into account a divergence angle of  $2^\circ$  during the 20 mm free flight. The guide tube curves gently ( $<3^\circ$ ) between the first and second expansion chambers to aim the pellet trajectory at the outer half radius of the plasma cross section.

## B. Differential pumping system

Removal of spent propellant gas is indispensable to apply the pneumatic type pellet injector to plasma experiments. For this purpose, a three-stage differential pumping system is provided. To secure effective pumping performance of the three-stage differential pumping system, large capacity backing vacuum pumps are installed. There are three systems of the backing vacuum pumps, two systems are exclusively for the pellet injector (roots pump station with pumping capacity of  $1800 \text{ m}^3/\text{h}$  and  $900 \text{ m}^3/\text{h}$ , respectively) and another is the common system of the LHD experiment.

In the three-stage differential pumping system, the volumes of the expansion chambers are  $0.23 \text{ m}^3$ ,  $0.23 \text{ m}^3$ , and  $0.07 \text{ m}^3$ , respectively. In each expansion chamber, an adequate type of vacuum pump is installed according to its own vacuum conditions. Types and effective pumping speed for helium gas of each vacuum pump are a helical groove pump ( $0.27 \text{ m}^3/\text{s}$ ), which has a wide operating range from ultrahigh vacuum to the viscous flow region at pressures above  $10^2 \text{ Pa}$ , and two turbo drag pumps ( $1.4 \text{ m}^3/\text{s}$  and  $0.3 \text{ m}^3/\text{s}$ ), respectively. Fig. 6(a) shows a conceptual diagram of the three-stage differential pumping system. The performance of the three-stage differential pumping system can be modeled by the following equations:

$$\begin{cases} V_1 \frac{dP_1}{dt} = I_{acc}\delta(t) + c_{12}(P_2 - P_1) - S_1P_1 + L_1, \\ V_2 \frac{dP_2}{dt} = c_{12}(P_1 - P_2) + c_{23}(P_3 - P_2) - S_2P_2 + L_2, \\ V_3 \frac{dP_3}{dt} = c_{23}(P_2 - P_3) - S_3P_3 + L_3, \end{cases} \quad (2)$$

where  $I_{acc}$ ,  $P_i$ ,  $V_i$ ,  $S_i$ ,  $C_{i(i+1)}$ , and  $L_i$  denote the propellant gas inflow rate, pressure of the stage  $i$ , volume of the stage  $i$ , pumping speed of the stage  $i$ , conductance between the stages  $i$  and  $i+1$ , and leak and/or degassing rate of the stage  $i$ , respectively. The conductance can be estimated by  $c = 330(d^3/\ell)$

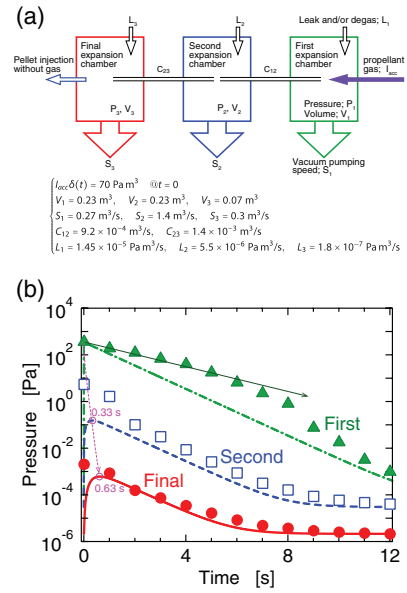


FIG. 6. Exhaust performance of the differential pumping system. (a) Conceptual diagram of the three-stage differential pumping system and the representative parameter of the system. (b) Comparison between the calculation results and measurements. Chain line, broken line, and solid line denote the calculated pressure change at the first, second, and final expansion chambers, respectively. Filled triangle, open square, and filled circle denote the measured pressure change at the first, second, and final expansion chambers, respectively.

in  $\text{m}^3/\text{s}$  assuming a molecular flow of helium gas at room temperature, where  $d$  and  $\ell$  are inner diameter and length of a tube in m. Differential pumping properties at launching a pellet are shown in Fig. 6(b). Calculated pressure changes in the expansion chambers are denoted by lines, and experimentally measured pressure changes are denoted by symbols. The model calculation result can reproduce the measured pressure in general. However, it must be noted that there are discrepancies just after launching the pellet. In the model calculation, there are time delays in increasing pressure in the second and third expansion chambers and the delay in the third expansion chamber (0.63 s) is longer than that in the second expansion chamber (0.33 s) due to the finite pressure propagation through the narrow guide tube. In contrast, the pressure rises are observed at the same time in all expansion chambers in the measured pressure. This phenomena can be explained by considering the direct gas admission from the upstream guide tube to the downstream one before the propellant gas expands isotropically into the expansion chamber at the gap, since the propellant gas has a large velocity component in the direction along the guide tube. In order to eliminate this non-ideal phenomena, extending the gap length should be one of the possible solutions although the adverse effects with the extension of free flight distance must be considered. Another point to note is that the observed rate of a pressure decrease in the first expansion chamber is relatively slow as compared with the calculated one especially in the high pressure region beyond 10 Pa. This phenomena shows pumping performance deterioration due to higher pressure, since the pumping speed of the helical groove pump shows deterioration at high pressure above 1 Pa although it is available for higher pressure

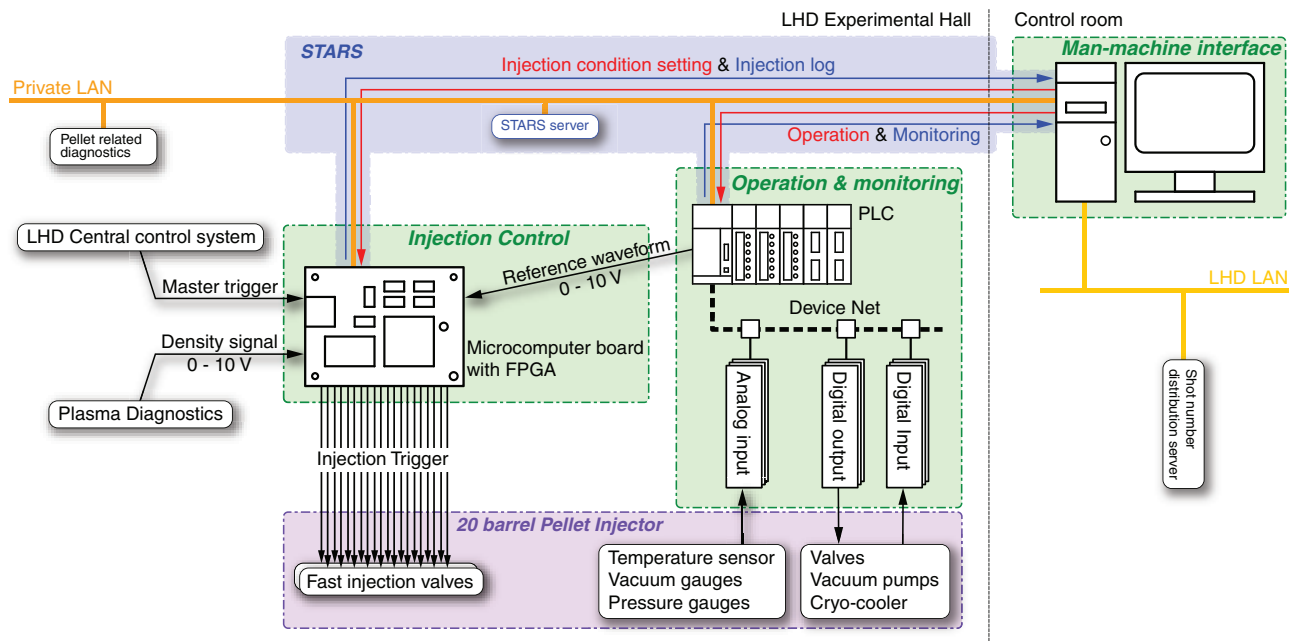


FIG. 7. Schematic diagram of the pellet injection control system which consists of three sections, (1) man-machine interface, (2) operation and monitoring, and (3) injection control. Each section is connected to the others through an Ethernet LAN connection.

up to 1000 Pa at which a normal turbo drag pump cannot be used. At the same time, maximum pressure in the third expansion chamber is approximately  $10^{-3}$  Pa and this pressure is the same level as that in the LHD vacuum vessel during the high density discharge. Therefore, the propellant gas does not flow into the LHD vacuum vessel effectively. It has been demonstrated that the performance of the three-stage differential pumping system is sufficient to use in the LHD experiment practically.

### C. Injector control system

The pellet injection control system consists of (1) man-machine interface section, (2) operation and monitoring section, and (3) injection control section, as shown in Fig. 7. These control sections communicate with each other using STARS (Simple Transmission and Retrieval System),<sup>16,17</sup> which is a message transferring middleware for small scale control systems with TCP/IP sockets. The operation of the pellet injector is fully automated by the control system and it is possible to inject 20 pellets per plasma discharge, which is repeated with a 3 min period, following the master trigger from the LHD central control system.

- (1) The man-machine interface section is a GUI (Graphical User Interface) program, which is developed in the Visual BASIC .NET, on the personal computer in the LHD central control room. The GUI programs consist of an injection condition setting program and an operational supervision program to collect and display the device status data. All the operation related to the pellet injection is conducted using GUI programs.
- (2) The operation and monitoring section consists of a PLC and data I/O components which communicate with the PLC using the DeviceNet.<sup>18</sup> There are approximately

100 channels of digital I/O to operate cryo-coolers, vacuum pumps and valves, and approximately 40 channels of analog I/O to measure temperatures and pressures. All procedures of the pellet injector operation and safety interlock are programmed in the PLC, and it can function automatically following instruction from the above-mentioned GUI programs.

- (3) Since the injection control section requires a high-speed response to perform real-time injection control, a microcomputer board, which is equipped with a FPGA (Field Programmable Gate Array), is employed. On the microcomputer board, a small scale UNIX system is running and C language programming is available. A real-time pellet injection timing control program consists of a digital logic program using VHDL (Very High speed integrated circuits Hardware Description Language) and a communicating interface program using C language.

There are two modes of pellet injection timing control. One is a pre-programmed mode in which all pellets are injected following previously defined times set by the injection condition setting program. Another is a real-time control mode in which pellet injection timings are defined in real time referring to a density related signal, e.g., interferometer or bremsstrahlung. The pre-set parameters are (i) the injection timing of arbitrary number of pellets (more than one) and (ii) the target density level, which is scaled to a voltage (1–10 V), as a function of time. Even in the real-time control mode, the first set of pellets is injected following a pre-set timing to build up a high density plasma. And then, real-time control of the pellet injection timing is activated to make the plasma density follow the previously defined target density as a function of time. A criterion for injecting pellets in the real-time control is the logical product of the following conditions: that the density related measurement value, which is scaled to

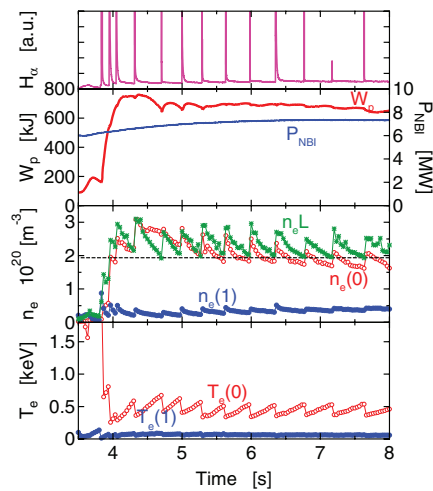


FIG. 8. Waveform of the pellet fueled discharge with real-time injection timing control to maintain  $n_e \ell = 2 \times 10^{20} \text{ m}^{-2}$  referring to a line density signal.

a voltage (1–10 V), is lower than the previously defined target value and the elapsed time from the last pellet injection is longer than 20 ms.

#### IV. FIRST APPLICATION AT LHD

The first application of the 20 barrel *in situ* pipe gun type solid hydrogen pellet injector has been carried out on LHD. Fig. 8 shows the waveform of the discharge (#104258). The first three pellets are injected following a pre-set timing and then pellet injection timing is controlled to keep the minimum line density at  $n_e \ell = 2 \times 10^{20} \text{ m}^{-2}$  in real time. The lower envelope of the line density is successfully kept constant as planned. However, it is interesting to note that the central density,  $n_e(0)$ , is gradually decreasing at the same time and the peripheral density,  $n_e(1)$ , is gradually increasing. The pellet injection interval to maintain the constant density at  $2 \times 10^{20} \text{ m}^{-2}$  becomes longer with time. These observations show that the sustainment of high density plasma with the massive pellet fueling leads to an unexpected increase of the peripheral density due to an increase of the recycling particles. In order to sustain high density plasma for a longer time, not only the effective core fueling by pellet injection but also active pumping capability at the divertor is essentially required, though this problem is beyond the scope of this paper.

#### V. SUMMARY

A 20 barrel solid hydrogen pellet injector, which is able to inject 20 cylindrical pellets with diameter and length of between 3.0 and 3.8 mm at the velocity of 1200 m/s, has been developed for the purpose of expanding the plasma operational regime to higher density and demonstrating the long duration sustainability of the high density plasma on LHD. In order to ensure stable operation as a fundamental facility in plasma experiments, which are performed every 3 min for 9 h each day, a simple *in situ* pneumatic pipe-gun concept is

employed and 20 barrels are arranged in parallel. Although a foremost concern of pneumatic pellet acceleration is the use of massive propellant gas, it is demonstrated that the propellant gas can be exhausted adequately using a three-stage differential pumping system with large capacity vacuum pumps. Real-time pellet injection timing control referring the density related measurements is developed by using a microcomputer board which is equipped with a FPGA, and it allows sustainment of high density plasma around the density limit avoiding a radiation collapse. The pellet injector has demonstrated stable operation characteristics in the plasma discharges beyond 2000 shots during the past three years of LHD experiments.

#### ACKNOWLEDGMENTS

This work is supported by Grant-in-Aid for Scientific Research (S) 20226018 and NIFS ULPP004.

<sup>1</sup>S. L. Milora, *Nucl. Fusion* **35**, 657 (1995).

<sup>2</sup>B. Pégourié, *Plasma Phys. Controlled Fusion* **49**, R87 (2007).

<sup>3</sup>S. K. Combs, *Rev. Sci. Instrum.* **64**, 1679 (1993).

<sup>4</sup>O. Motojima, H. Yamada, A. Komori, N. Ohya, K. Kawahata, O. Kaneko, S. Masuzaki, A. Ejiri, M. Emoto, H. Funaba, M. Goto, K. Ida, H. Idei, S. Inagaki, N. Inoue, S. Kado, S. Kubo, R. Kumazawa, T. Minami, J. Miyazawa, T. Morisaki, S. Morita, S. Murakami, S. Muto, T. Mutoh, Y. Nagayama, Y. Nakamura, H. Nakanishi, K. Narihara, K. Nishimura, N. Noda, T. Kobuchi, S. Ohdachi, Y. Oka, M. Osakabe, T. Ozaki, B. J. Peterson, A. Sagara, S. Sakakibara, R. Sakamoto, H. Sasao, M. Sasao, K. Sato, M. Sato, T. Seki, T. Shimozuma, M. Shoji, H. Suzuki, Y. Takeiri, K. Tanaka, K. Toi, T. Tokuzawa, K. Tsumori, K. Tsuzuki, I. Yamada, S. Yamaguchi, M. Yokoyama, K. Y. Watanabe, T. Watari, Y. Hamada, K. Matsuoka, K. Murai, K. Ohkubo, I. Ohtake, M. Okamoto, S. Satoh, T. Satow, S. Sudo, S. Tanahashi, K. Yamazaki, M. Fujiwara, and A. Iiyoshi, *Phys. Plasmas* **6**, 1843 (1999).

<sup>5</sup>N. Ohya, T. Morisaki, S. Masuzaki, R. Sakamoto, M. Kobayashi, J. Miyazawa, M. Shoji, A. Komori, O. Motojima, and LHD Experimental Group, *Phys. Rev. Lett.* **97**, 055002 (2006).

<sup>6</sup>R. Sakamoto, M. Kobayashi, J. Miyazawa, S. Ohdachi, H. Yamada, H. Funaba, M. Goto, S. Masuzaki, T. Morisaki, I. Yamada, K. Narihara, K. Tanaka, S. Morita, K. Ida, S. Sakakibara, Y. Narushima, K. Y. Watanabe, Y. Suzuki, N. Ashikawa, Y. Nagayama, B. J. Peterson, M. Shoji, C. Suzuki, M. Tokitani, S. Yoshimura, N. Ohya, A. Komori, O. Motojima, and LHD Experimental Group, *Nucl. Fusion* **49**, 085002 (2009).

<sup>7</sup>M. Hoshino, R. Sakamoto, H. Yamada, R. Kumazawa, T. Watari, and LHD Experimental Group, *Fusion Eng. Des.* **81**, 2655 (2006).

<sup>8</sup>R. Sakamoto, H. Yamada, and LHD Experimental Group, *Plasma Fusion Res.* **4**, 002 (2009).

<sup>9</sup>J. Urbahn, M. Greenwald, and J. Schachter, in *Proceedings of the 15th IEEE/NPSS Symposium on Fusion Engineering* (IEEE, 1993), Vol. 1, p. 44.

<sup>10</sup>J. Lafferrandier, G. Claudet, and F. Disdier, in *Proceedings of the 14th Symposium on Fusion Technology* (Pergamon Press, 1986), Vol. II, p. 1367.

<sup>11</sup>H. Yamada, R. Sakamoto, Y. Oda, T. Hiramatsu, M. Kinoshita, M. Ogino, R. Matsuda, S. Sudo, S. Kato, P. W. Fisher, L. R. Baylor, and M. Gouge, *Fusion Eng. Des.* **49–50**, 915 (2000).

<sup>12</sup>P. B. Parks and R. J. Turnbull, *Phys. Fluids* **21**, 1735 (1978).

<sup>13</sup>J. S. Mishra, R. Sakamoto, G. Motojima, A. Matsuyama, and H. Yamada, *Rev. Sci. Instrum.* **82**, 023505 (2011).

<sup>14</sup>R. Sakamoto and H. Yamada, *NIFS Research Reports*, NIFS-TECH Series Vol. 13 (NIFS, 2005), see <http://www.nifs.ac.jp/report/nifs-tech13.html>.

<sup>15</sup>L. D. Landau and E. M. Lifshitz, *Fluid Mechanics* (Pergamon Press, 1987).

<sup>16</sup>T. Kosuge, K. Nigorikawa, Y. Nagatani, and Y. Saito, *AIP Conf. Proc.* **1234**, 701 (2010).

<sup>17</sup>Photon Factory, IMSS, KEK, see <http://stars.kek.jp/index.html>.

<sup>18</sup>Open DeviceNet Vendors Association, see <http://www.odva.org>.